

Progress of Theoretical Physics, Vol. 54, No. 6, December 1975

## The Unrestricted Hartree-Fock Theory of Chemical Reactions. V

—The Reaction of Three Hydrogens in Isosceles  
Triangular Conformations—

Kizashi YAMAGUCHI\* and Hideo FUKUTOME

\**Department of Chemistry, Faculty of Engineering Science, Osaka University  
Toyonaka, Osaka*

*Department of Physics, Kyoto University, Kyoto*

(Received March 3, 1975)

A UHF theoretical analysis is carried out for the reaction of three hydrogens in isosceles triangular conformations. It is shown that the UHF ground state of the  $H_3$  system consists of three different "electronic phases"; an RHF configuration in a region of acute triangles, an ASDW configuration in a region of flat triangles and a TSDW configuration in a region near equilateral triangles. The potentials of the UHF states are calculated and their interconnection relation is studied. A configurational analysis in terms of the RHF orbitals is carried out for the UHF states at equilateral triangles. It is shown that the TSDW state is a good approximation to the full CI ground state. The reason for the missing of the Jahn-Teller cusp in the UHF ground state potential is discussed. Importance of spin flipping instabilities in mechanistic characterization of radical reactions is pointed out.

### § 1. Introduction

In previous papers,<sup>1-5)</sup> we have carried out unrestricted Hartree-Fock (UHF) theoretical analyses of the chemical reactions in singlet ground state. We consider, in this paper, the three hydrogen system with isosceles triangular conformations as one of the simplest model system for insertion reactions of free radicals. We show from an analysis of the  $H_3$  system that instability of a ground state configuration and appearance of a new ground state of broken symmetry character are phenomena which may occur not only in the reacting systems with a singlet ground state but also in the systems with a doublet ground state, i.e., in free radical reactions. The UHF ground state of the  $H_3$  system undergoes "electronic phase transitions" between a restricted Hartree-Fock (RHF), an axial spin density wave (ASDW) and a torsional spin density wave (TSDW) configurations, indicating the presence of a hierarchy of doublet radicals with electronic structures of increasing complexities as in singlet radicals discussed previously.<sup>6)</sup> A configurational analysis is carried out for the ASDW and the TSDW states at equilateral triangles in order to clarify the nature of the electronic correlation effects incorporated into the UHF states.

The reason for the missing of the Jahn-Teller cusp<sup>6)</sup> in the UHF ground state

potential is discussed in connection with the configurational analysis.

We use, in this paper, the notation for the types of UHF solutions and their instabilities developed in other papers on the UHF equation.<sup>7,8)</sup> We use the CNDO approximation<sup>9)</sup> in all calculations in this paper. Computations were carried out on a FACOM 230-60 computer at the Computer Center, of Kyoto University.

## § 2. Doublet UHF configurations in isosceles triangular $H_3$ system and their instabilities

We consider the insertion process of a hydrogen atom toward a hydrogen molecule in the reaction path with isosceles triangular conformations ( $C_{2v}$  symmetry) illustrated by Fig. 1(a). The symmetry-adapted RHF orbitals of the  $H_3$  radical in the minimal basis approximation are determined by the  $C_{2v}$  symmetry of the system as

$$\left. \begin{aligned} \phi_a &= \cos \frac{\theta}{2} \psi_a + \sin \frac{\theta}{2} \psi_a', \\ \phi_a' &= -\sin \frac{\theta}{2} \psi_a + \cos \frac{\theta}{2} \psi_a', \\ \phi_b &= \psi_b, \end{aligned} \right\} \quad (2.1)$$

where  $\theta$  is a variation parameter and the basis functions are expressed with the orthogonalized atomic 1s orbitals  $\chi_i$  ( $i=1, 2, 3$ ) as

$$\left. \begin{aligned} \psi_a &= \frac{1}{\sqrt{2}}(\chi_1 + \chi_2), \\ \psi_a' &= \chi_3, \\ \psi_b &= \frac{1}{\sqrt{2}}(\chi_1 - \chi_2). \end{aligned} \right\} \quad (2.2)$$

The orbitals  $\phi_a'$  and  $\phi_b$  become degenerate at equilateral triangular ( $D_{3h}$ ) con-

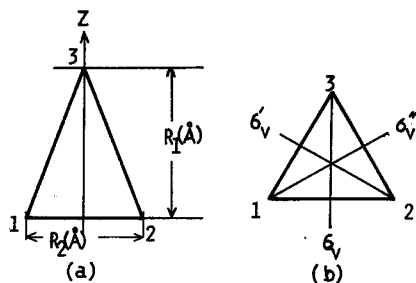


Fig. 1. The geometry of the  $H_3$  system with  $C_{2v}$  symmetry (a) and  $D_{3h}$  symmetry (b).

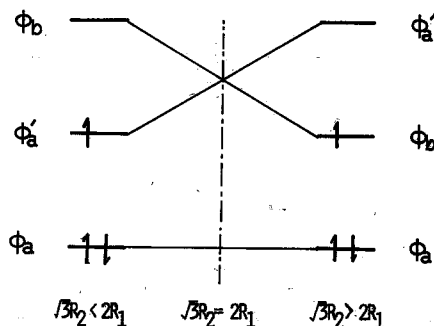


Fig. 2. Orbital correlation diagram of the  $H_3$  system.

formations, making an  $E'$  representation of  $D_{3h}$  group. Therefore, a crossing of the orbitals occurs in the course of the insertion process as illustrated by the orbital correlation diagram in Fig. 2. As is apparent from Fig. 2, the configuration  $|\phi_a\bar{\phi}_a\phi_{a'}|$ , which we denote  $RHF_1$ , is lower in energy than the configuration  $|\phi_a\bar{\phi}_a\phi_b|$ ,  $RHF_2$ , in acute triangle conformations ( $\sqrt{3}R_2 < 2R_1$ ).  $RHF_2$ , on the other hand, becomes lower in energy than  $RHF_1$  in flat triangle conformations ( $\sqrt{3}R_2 > 2R_1$ ).

As shown by Paldus and Čížek<sup>10</sup> and by one of the authors,<sup>9</sup> the first order variation for the energy of a doublet RHF configuration does not necessarily disappear and it is not necessary a solution of the UHF equation. In fact,  $RHF_2$  is not a solution of the UHF equation because of the nonzero first order variation which is given by the integral  $\langle \phi_a\phi_b | \phi_b\phi_{a'} \rangle$ . This indicates that the spin polarization effect always contributes to the energetic stabilization in the flat  $H_3$  radical and an ASDW solution, which we call  $ASDW_2$ , lower in energy than  $RHF_2$  should exist.

Due to the crossing of the RHF orbitals  $\phi_{a'}$  and  $\phi_b$ ,  $RHF_1$  becomes unstable for the antisymmetric spin flipping excitations  $\phi_{a'}\eta_+ \rightarrow \phi_b\eta_-$  and  $\phi_a\eta_- \rightarrow \phi_b\eta_+$  in a region near equilateral triangles. We show in Fig. 3 the  $A_M$  instability boundary  $T_1$  of  $RHF_1$ . It is stable in the region I of acute triangles, but becomes  $A_M$  unstable in the region beyond the boundary  $T_1$ . It becomes unstable also for the antisymmetric spin unflipping excitations  $\phi_{a'}\eta_{\pm} \rightarrow \phi_b\eta_{\pm}$  and  $\phi_a\eta_{\pm} \rightarrow \phi_b\eta_{\pm}$ . The  $A_+M_+$  instability of  $RHF_1$  occurs at a boundary which is very close to the boundary  $T_1$  of the  $A_M$  instability and only a little nearer to equilateral triangles, so we do not show it in Fig. 3. The occurrence of  $A_M$  and  $A_+M_+$  instabilities in  $RHF_1$  indicates that there are a TSDW and an ASDW configurations lower in energy

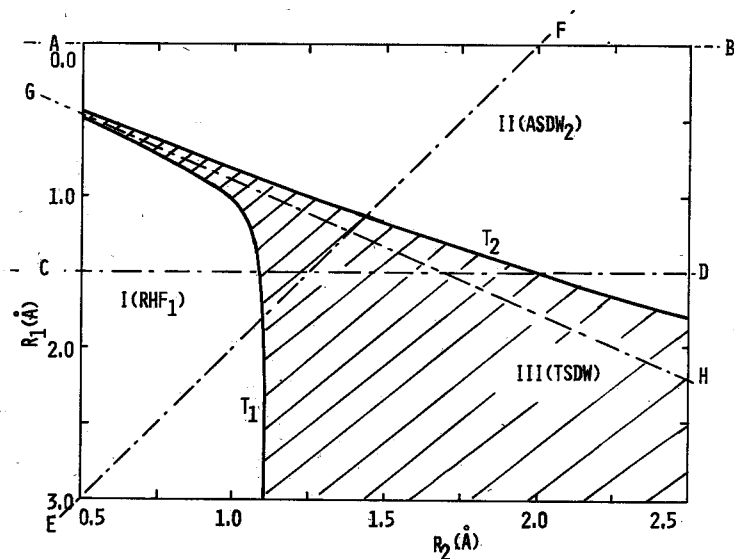


Fig. 3. The  $A_M$  instability boundaries for  $RHF_1$  ( $T_1$ ) and  $ASDW_2$  ( $T_2$ ). The hatched region is the domain of the TSDW ground state. The line GH represents equilateral triangles.

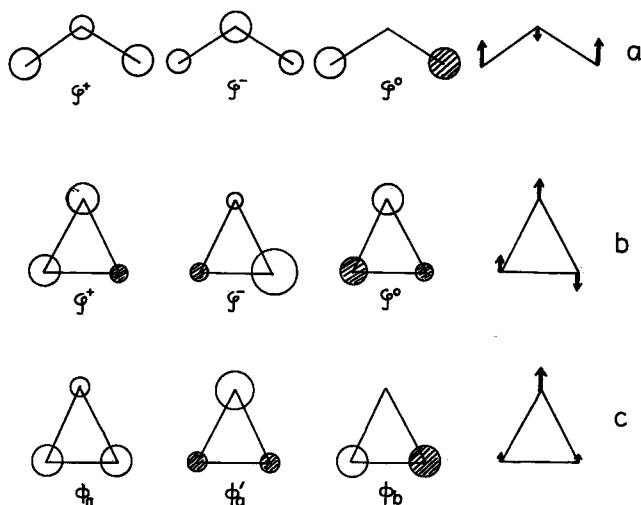


Fig. 4. Schematic representations for the orbitals of ASDW<sub>2</sub> (a), ASDW<sub>1</sub> (b) and RHF<sub>1</sub> (c). The white circle represents the MO coefficients with positive sign and the shaded one that with negative sign. The spin structures of the states are also indicated at right.

than RHF<sub>1</sub> in the regions beyond the instability boundaries. We call the ASDW configuration emerging from the  $A_+M_+$  instability of RHF<sub>1</sub> as ASDW<sub>1</sub>.

The excitations bringing the non-zero first order variation of RHF<sub>2</sub> are the spin unflipping symmetric transitions  $\phi_a\eta_{\pm} \rightarrow \phi_a'\eta_{\pm}$ . Therefore the spin polarized orbitals of the ASDW<sub>2</sub> configuration for the flat  $H_3$  radical are constructed with a mixing between the occupied and virtual RHF orbitals  $\phi_a$  and  $\phi_a'$  as

$$\left. \begin{aligned} \varphi_{\text{ASDW}_2}^{\pm} &= \left( \cos \frac{\omega^{\pm}}{2} \phi_a + \sin \frac{\omega^{\pm}}{2} \phi_a' \right) \eta_{\pm}, \\ &= (b_1^{\pm} \phi_a + b_2^{\pm} \phi_a') \eta_{\pm}, \\ \varphi_{\text{ASDW}_2}^0 &= \phi_b \eta_{\pm}, \\ b_1^{\pm} &= \cos(\omega^{\pm} + \theta) / 2, \quad b_2^{\pm} = \sin(\omega^{\pm} + \theta) / 2. \end{aligned} \right\} \quad (2.3)$$

The ASDW<sub>2</sub> orbitals are  $C_{2v}$  symmetry-adapted, as illustrated in Fig. 4(a), because they are constructed from the RHF orbitals of the same symmetry. The ASDW<sub>1</sub> orbitals for the acute  $H_3$  radical, on the other hand, can be constructed with a mixing between the symmetric and antisymmetric RHF orbitals because ASDW<sub>1</sub> emerges from the  $A_+M_+$  instability of RHF<sub>1</sub> caused by the antisymmetric excitations  $\phi_a'\eta_{+} \rightarrow \phi_b\eta_{+}$  and  $\phi_a\eta_{\pm} \rightarrow \phi_b\eta_{\pm}$ ;

$$\left. \begin{aligned} \varphi_{\text{ASDW}_1}^{\pm} &= (a_1^{\pm} \phi_a + a_2^{\pm} \phi_a' + a_3^{\pm} \phi_b) \eta_{\pm}, \\ \varphi_{\text{ASDW}_1}^0 &= (a_1 \phi_a + a_2 \phi_a' + a_3 \phi_b) \eta_{\pm}, \end{aligned} \right\} \quad (2.4)$$

where  $a_i^{\pm}$  and  $a_i$  are real coefficients satisfying

$$\sum_i (a_i^{\pm})^2 = \sum_i (a_i)^2 = 1, \quad \sum_i a_i^+ a_i = 0.$$

The ASDW<sub>1</sub> orbitals are of broken  $C_{2v}$  symmetry as illustrated in Fig. 4(b). In

the limit  $a_3^\pm = a_3 = 0$ , they reduce to the RHF<sub>1</sub> orbitals which are also depicted in Fig. 4(c).

The atomic spin densities in the ASDW<sub>2</sub> and the ASDW<sub>1</sub> configurations are given by

$$\left. \begin{aligned} S_{1z} = S_{2z} = \frac{1}{2} [(b_1^+)^2 - (b_1^-)^2 - 1], \\ S_{3z} = (b_2^+)^2 - (b_2^-)^2, \end{aligned} \right\} \text{ for ASDW}_2, \quad (2.5)$$

$$\left. \begin{aligned} S_{1z} = \frac{1}{2} (A_1 + A_2), \\ S_{2z} = \frac{1}{2} (A_1 - A_2), \\ S_{3z} = (a_2^+)^2 - (a_2^-)^2 + a_2^2, \end{aligned} \right\} \text{ for ASDW}_1, \quad (2.6)$$

where

$$A_1 = (a_1^+)^2 - (a_1^-)^2 + (a_3^+)^2 - (a_3^-)^2 + a_1^2 + a_3^2,$$

$$A_2 = a_1^+ a_3^+ - a_1^- a_3^- + a_1 a_3.$$

The  $x$  and  $y$  components of the spin density are always zero in ASDW<sub>1</sub> and ASDW<sub>2</sub>. The spin structures of the RHF<sub>1</sub>, ASDW<sub>1</sub> and ASDW<sub>2</sub> configurations are also illustrated in Fig. 4.

ASDW<sub>2</sub> is  $A_-M$ -stable in flat triangles near linear conformations. However, it becomes unstable for the spin flipping antisymmetric excitations in a region near  $D_{3h}$  conformations. We show in Fig. 3 the  $A_-M$  instability boundary  $T_2$  of ASDW<sub>2</sub>. ASDW<sub>2</sub> is  $A_+M_+$  stable in the whole region  $\sqrt{3}R_2 > 2R_1$  of flat triangles, so it is the lowest energy ASDW configuration there but a TSDW configuration of lower energy exists in the region beyond the  $A_-M$  instability boundary  $T_2$ .

ASDW<sub>1</sub>, on the other hand, is always  $A_-M$  unstable. This is due to the existence of a TSDW solution emerging from the  $A_-M$  instability of RHF<sub>1</sub> prior to the emergence of ASDW<sub>1</sub>. However, it is always  $A_+M_+$  stable in the region  $\sqrt{3}R_2 < 2R_1$  of acute triangles, indicating that it is the lowest energy ASDW configuration there.

Thus, RHF<sub>1</sub> and ASDW<sub>2</sub> are the ground state in the regions I and II of acute and flat triangles respectively, but a TSDW configuration should be the ground state in the region III near equilateral triangles as depicted in Fig. 3. We see from Fig. 3 that no change in the ground state nature takes place in the dissociation process of the linear  $H_3$  radical along the path AB but the character of the ground state changes in the insertion process of an  $H$  atom into an  $H_2$  molecule. Any reaction path of the insertion process traverses the region of TSDW ground state in the vicinity of equilateral triangular conformations.

At equilateral triangles with  $D_{3h}$  symmetry, the RHF orbitals become

$$\left. \phi_a = \sqrt{\frac{2}{3}} \psi_a + \frac{1}{\sqrt{3}} \psi'_a = \frac{1}{\sqrt{3}} (\chi_1 + \chi_2 + \chi_3), \right\}$$

$$\left. \begin{aligned} \phi_a' &= \frac{1}{\sqrt{3}}\phi_a + \sqrt{\frac{2}{3}}\phi_a' = \frac{1}{\sqrt{6}}(2\chi_3 - \chi_1 - \chi_2), \\ \phi_b &= \phi_b = \frac{1}{\sqrt{2}}(\chi_1 - \chi_2). \end{aligned} \right\} \quad (2.7)$$

The orbitals of ASDW<sub>1</sub> at  $D_{3h}$  conformations can be expressed as

$$\left. \begin{aligned} \varphi_{\text{ASDW}_1}^{\pm} &= \left\{ \phi_a \cos \frac{\omega^{\pm}}{2} - \frac{1}{2}(\phi_a' + \sqrt{3}\phi_b) \sin \frac{\omega^{\pm}}{2} \right\} \eta_{\pm}, \\ \varphi_{\text{ASDW}_1} &= \frac{1}{2}(-\sqrt{3}\phi_a' + \phi_b) \eta_+, \end{aligned} \right\} \quad (2.8)$$

with the same parameters  $\omega^{\pm}$  as ASDW<sub>2</sub>. From the relations

$$\left. \begin{aligned} -\frac{1}{2}(\phi_a' + \sqrt{3}\phi_b) &= \frac{1}{\sqrt{6}}(2\chi_2 - \chi_1 - \chi_3), \\ \frac{1}{2}(-\sqrt{3}\phi_a' + \phi_b) &= \frac{1}{\sqrt{2}}(\chi_1 - \chi_3), \end{aligned} \right\} \quad (2.9)$$

we see that ASDW<sub>1</sub> at  $D_{3h}$  is symmetry adapted to the  $C_{2v}$  operations around the axis  $\sigma_v'$  defined in Fig. 1(b) while ASDW<sub>2</sub> is symmetry adapted to the  $C_{2v}$  operations around the axis  $\sigma_v$ . The symmetries of ASDW<sub>1</sub> and ASDW<sub>2</sub> lead to their degeneracy at  $D_{3h}$  conformations.

Since the TSDW ground state near equilateral triangles emerges from the  $A_M$  instabilities of  $C_{2v}$  symmetry adapted RHF<sub>1</sub> and ASDW<sub>2</sub> for the spin flipping antisymmetric excitations, its orbitals should be constructed with a mixing of the symmetric and antisymmetric spin orbitals with opposite directions of spin:

$$\left. \begin{aligned} \varphi_{\text{TSDW}}^{\pm} &= (c_1^{\pm}\phi_a + c_2^{\pm}\phi_a') \eta_{\pm} + c_3^{\pm}\phi_b \eta_{\mp}, \\ \varphi_{\text{TSDW}} &= (c_1\phi_a + c_2\phi_a') \eta_+ + c_3\phi_b \eta_-, \end{aligned} \right\} \quad (2.10)$$

where  $c_i^{\pm}$  and  $c_i$  are real coefficients satisfying

$$\sum_i (c_i^{\pm})^2 = \sum_i c_i^2 = 1, \quad \sum_i c_i^+ c_i = 0.$$

The atomic spin density in the  $M_y$ -invariant TSDW state (2.10) is modulated in the  $(x, z)$  plane and given by

$$\left. \begin{aligned} S_{1x} &= a, & S_{1z} &= b, \\ S_{2x} &= -a, & S_{2z} &= b, & S_{iy} &= 0, \\ S_{3x} &= 0, & S_{3z} &= c, \end{aligned} \right\} \quad (2.11)$$

with

$$\left. \begin{aligned} a &= c_1^+ c_3^+ + c_1^- c_3^- + c_1 c_3, \\ b &= \frac{1}{2} \{ (c_1^+)^2 - (c_1^-)^2 - (c_3^+)^2 + (c_3^-)^2 + c_1^2 - c_3^2 \}, \\ c &= (c_2^+)^2 - (c_2^-)^2 + c_2^2. \end{aligned} \right\} \quad (2.12)$$

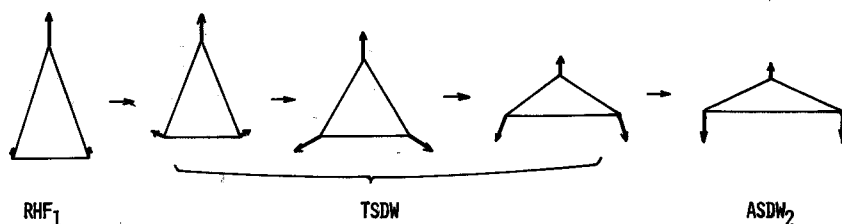


Fig. 5. The way of interconnection of  $RHF_1$  and  $ASDW_2$  wavefunctions via the TSDW state represented by their spin structures.

The spin structure of the TSDW state is ordered to  $C_{2v}$  group<sup>5)</sup> as illustrated in Fig. 5.

The TSDW solution (2.10) at equilateral triangles becomes an ordered spin solution to the  $D_{3h}$  group and its orbitals and spin structure are determined by a single parameter  $\mu$  as

$$\left. \begin{aligned} \varphi_{\text{TSDW}}^{\pm} &= \left( \phi_a \cos \frac{\mu}{2} + \frac{1}{2} (\sigma_3 \phi_a' + \sigma_1 \phi_b) \sin \frac{\mu}{2} \right) \eta_{\pm}, \\ \varphi_{\text{TSDW}} &= \frac{1}{\sqrt{2}} (\phi_a' \eta_+ - \phi_b \eta_-), \end{aligned} \right\} \quad (2.13)$$

$$\frac{2}{\sqrt{3}} a = -2b = c = \frac{1}{3} (1 + 2 \sin \mu). \quad (2.14)$$

The TSDW spin structure at  $D_{3h}$  conformations is the so-called triangular spin arrangement with the spin density vectors at the atomic sites 1, 2 and 3 rotating around the  $y$  axis consecutively by  $120^\circ$ , in the  $(x, z)$  plane.

The electronic energy of the TSDW state at equilateral triangles is given by

$$E_{\text{TSDW}} = 3\alpha + 3\beta \cos \mu + \frac{2}{3} \gamma_{11} + \frac{7}{3} \gamma_{12} - \frac{1}{3} (\gamma_{11} - \gamma_{12}) (\sin \mu + \sin^2 \mu), \quad (2.15)$$

where  $\alpha$  and  $\beta$  are the customary Coulomb and resonance integrals, respectively and  $\gamma_{11}$  and  $\gamma_{12}$  are the one and two center Coulomb repulsion integrals, respectively.

The TSDW orbital (2.10) reduces to the  $RHF_1$  and the  $ASDW_2$  orbitals at the  $A-M$  instability boundaries  $T_1$  and  $T_2$ , respectively:

$$\left. \begin{aligned} c_3^{\pm} = c_3 = 0, & \quad \text{at } T_1 \\ c_3^{\pm} = c_1 = c_2 = 0, & \quad \text{at } T_2 \end{aligned} \right\} \quad (2.16)$$

We show in Fig. 5 how the TSDW state interconnects  $RHF_1$  and  $ASDW_2$ . The axial spin structures of  $RHF_1$  and  $ASDW_2$  are smoothly connected through the torsional spin structure of the TSDW state. All the spin structures of the  $RHF_1$ ,  $ASDW_2$  and TSDW states are ordered to the  $C_{2v}$  group and this makes possible to interconnect them smoothly. The spin structures of  $ASDW_1$ , on the other hand, is not ordered to the  $C_{2v}$  group and it cannot be interconnected to the TSDW state.

We calculated the adiabatic potentials of  $\text{RHF}_1$ ,  $\text{ASDW}_1$  and  $\text{ASDW}_2$  using a usual DODS (different orbitals for different spins) type UHF CNDO computer program and feeding into it the trial orbitals with the forms of (2.1), (2.4) and (2.3), respectively. The potentials of the TSDW state was calculated by a UHF CNDO computer program adapted to GSO (generalized spin orbital) type solution by feeding into it the trial orbital in the form of (2.10). We show in Fig. 6 the adiabatic potentials of the UHF states along the paths AB, CD, EF and GH depicted in Fig. 3. As seen in Fig. 6, the  $\text{RHF}_1$ ,  $\text{ASDW}_2$  and TSDW states are the ground state in the regions I, II and III, respectively.  $\text{ASDW}_1$  is always higher in energy than the TSDW state and cannot be a ground state. The potentials of  $\text{ASDW}_1$  and  $\text{ASDW}_2$  cross at  $D_{3h}$  conformations. The TSDW potential segregates from  $\text{RHF}_1$  and  $\text{ASDW}_2$  and interconnect them continuously. In the insertion process EF, a potential barrier exists in the region III and the transition state lies at a conformation shifted from an equilateral triangle to a slightly acute one in agreement with other calculations.<sup>11)</sup> In the dissociation process of the equilateral  $H_3$  radical along the path GH, the  $\text{RHF}$  potential shows an incorrect asymptotic behavior but those of the  $\text{ASDW}$  and TSDW states converge to the correct limit of three  $H$  atoms. The true ground state of the  $H_3$  radical should show a Jahn-Teller behavior at  $D_{3h}$  conformations since it is an  $E'$  representation of  $D_{3h}$  group and degenerate. However, the TSDW ground state potential does not have a Jahn-Teller cusp at  $D_{3h}$  but changes continuously there. The reason for the missing of the Jahn-Teller cusp in the TSDW state shall be discussed in the next section.

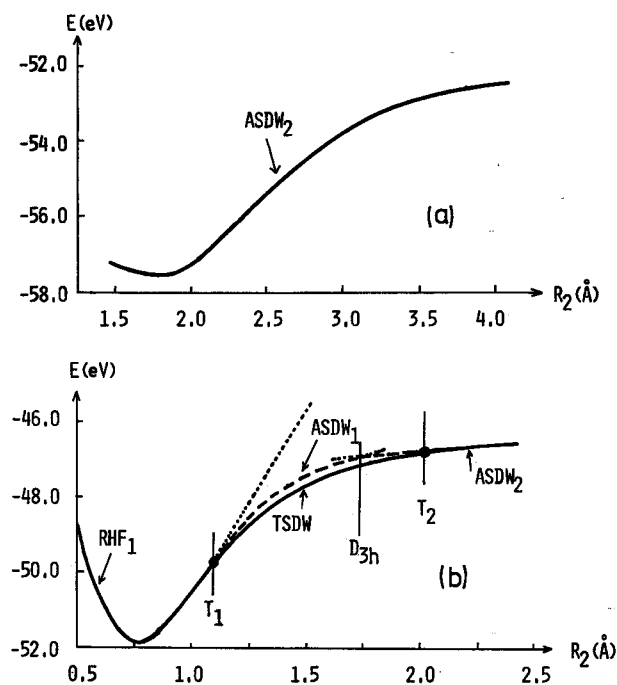


Figure captions are printed on the next page below.



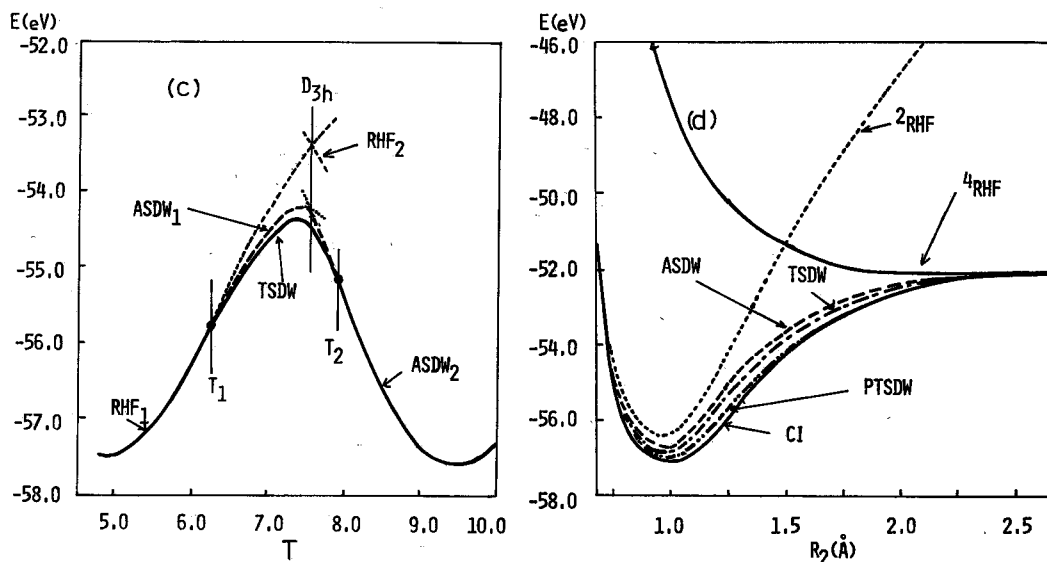


Fig. 6. The potentials of the UHF states on the lines AB (a), CD (b), EF (c) and GH (d) depicted in Fig. 3. The geometries of the insertion process (c) are given by the parameter  $T$ :  $R_1=0.50(10-T)$ ,  $R_2=0.25(T-2)$ . In the case of (d) for equilateral triangles, the potentials of the full CI state, the PTSDW state and the quartet state are also indicated.

### § 3. Configurational analysis on the ASDW and the TSDW states at equilateral triangles

In order to see the relations of the ASDW and the TSDW states to the exact doublet ground state constructed with a full configuration interaction (CI), we carry out a configurational analysis in terms of the RHF orbitals on the ASDW and the TSDW wavefunctions at equilateral triangles where the high  $D_{3h}$  symmetry makes it relatively easy. The exact ground state at equilateral triangles belongs to an  $E'$  representation of  $D_{3h}$  group and its wavefunction in the minimal basis approximation is given in a CI form as

$${}^2\Phi_0 = C_1|\phi_a\bar{\phi}_a\phi_e| + C_2|\phi_{-e}\bar{\phi}_{-e}\phi_a| + C_3|\phi_e\bar{\phi}_e\phi_{-e}|, \quad (3.1)$$

by using the complex RHF orbitals of  $E'$ -symmetry

$$\left. \begin{aligned} \phi_e &= \frac{1}{\sqrt{2}}(\phi_a' + i\phi_b) = \frac{1}{\sqrt{3}}(\chi_3 + \omega\chi_1 + \omega^2\chi_2), \\ \phi_{-e} &= \frac{1}{\sqrt{2}}(\phi_a' - i\phi_b) = \frac{1}{\sqrt{3}}(\chi_3 + \omega^2\chi_1 + \omega\chi_2), \end{aligned} \right\} \quad (3.2)$$

where  $\omega = \exp(2\pi i/3)$  and the  $C_i$ 's are normalized CI coefficients. The  $R_2$  dependence of the total energy of the exact ground state is shown in Fig. 6(d). We see that the TSDW potential is a good approximation to the exact ground state

potential.

To compare the TSDW wavefunction with that of the exact ground state, it is convenient to transform the  $M_y$ -invariant TSDW orbitals (2.13) into an  $M_z$ -invariant representation. Operating a spin rotation carrying the  $y$ -axis into the  $z$ -axis on (2.13), we obtain an  $M_z$ -invariant representation of the TSDW orbitals as

$$\left. \begin{aligned} \phi_{\text{TSDW}}^{\pm} &= \phi_a \cos \frac{\mu}{2} \eta_{\pm} + \phi_{\pm e} \sin \frac{\mu}{2} \eta_{\mp}, \\ \phi_{\text{TSDW}}^0 &= \frac{1}{\sqrt{2}} (\phi_e \eta_+ + \phi_{-e} \eta_-). \end{aligned} \right\} \quad (3.3)$$

The Slater determinant  $\Phi_{\text{TSDW}} = |\varphi^+ \varphi^- \varphi^0|$  of the TSDW solution is neither an eigenstate of  $S^2$  nor that of  $S_z$  ( $S$  being the total spin). Using (3.3), we see that it is an equal weighted sum of the wavefunctions with positive and negative  $S_z$ :

$$\left. \begin{aligned} \Phi_{\text{TSDW}} &= \frac{1}{\sqrt{2}} (\Phi_{\text{TSDW}}^+ + \Phi_{\text{TSDW}}^-), \quad \Phi_{\text{TSDW}}^- = M_z \Phi_{\text{TSDW}}^+, \\ \Phi_{\text{TSDW}}^{\pm} &= \frac{1}{2} \{ (1 + \cos \mu) |\phi_a \bar{\phi}_a \phi_e| + (1 - \cos \mu) |\phi_e \bar{\phi}_e \phi_{-e}| \\ &\quad + \sin \mu (|\phi_{-e} \bar{\phi}_{-e} \phi_a| + |\phi_a \phi_{-e} \phi_e|) \}, \end{aligned} \right\} \quad (3.4)$$

where the operation  $M_z$  consists of complex conjugation and the conversion of up and down spin eigenfunctions to down and up spin ones, respectively.  $\Phi_{\text{TSDW}}^{\pm}$  contains the doublet and the quartet components and we obtain from (3.4) the doublet projected TSDW (PTSDW) wavefunction as

$${}^2\Phi_{\text{PTSDW}} = \{ (1 + \cos \mu) |\phi_a \bar{\phi}_a \phi_e| + \sin \mu |\phi_{-e} \bar{\phi}_{-e} \phi_a| + (1 - \cos \mu) |\phi_e \bar{\phi}_e \phi_{-e}| \} (3 + \cos^2 \mu)^{-1/2}. \quad (3.5)$$

Equation (3.5) indicates that the PTSDW wavefunction is of the same form as (3.1) with the CI coefficients

$$\left. \begin{aligned} C_1 &= N(1 + \cos \mu), \quad C_2 = N \sin \mu, \quad C_3 = N(1 - \cos \mu), \\ N &= (3 + \cos^2 \mu)^{-1/2}, \end{aligned} \right\} \quad (3.6)$$

and is of  $E'$ -symmetry in  $D_{3h}$  group correctly representing the symmetry of the ground state. The exact CI wavefunction (3.1) contains two independent CI parameters but the PTSDW state only a parameter  $\mu$ , so that the energy of the PTSDW state is always higher than the exact CI state. We obtain from (3.4) and (3.5) the energy of the PTSDW state as

$${}^2E_{\text{PTSDW}} = (4E_{\text{TSDW}} - \sin^2 \mu {}^4E_{\text{RHF}}) / (3 + \cos^2 \mu). \quad (3.7)$$

where  ${}^4E_{\text{RHF}} = 3\alpha + 3\gamma_{12}$  is the energy of the quartet RHF state  $|\phi_a \phi_a' \phi_b|$  at equilateral triangles.

We show in Fig. 6(d) also the potential of the PTSDW state calculated with (3.7). It is apparent that the PTSDW potential is an excellent approximation to the exact ground state potential. We compare in Fig. 7 the CI coefficients (3.6) in the PTSDW state with those in the exact ground state. As is apparent in Fig. 7, the PTSDW wavefunction is an excellent approximation to the exact CI wavefunction in the whole range of  $R_2$ . The weights of the ground configuration in the exact CI state is always a little smaller than that in the PTSDW state, indicating that the total weight of the doubly excited configurations is somewhat underestimated in the PTSDW state.

The equilateral  $H_3$  radical has the character of a monoradical at small interatomic distances since the weight  $C_1^2$  of the ground RHF configuration is dominant there. However, at large interatomic distances, it dissociates into three hydrogen atoms, having the character of a tri-radical. As seen in Fig. 7, the weight  $C_1^2$  decreases rapidly with increase of  $R_2$ , the weights  $C_2^2$  and  $C_3^2$  of the two doubly excited RHF configurations increase and the three RHF configurations mix with equal weights in the dissociation limit. Singlet diradicals have been characterized to have CI wavefunctions with a heavy mixing of a doubly excited configuration.<sup>12), 13)</sup> From the present result and the characterization of diradicals, it may be plausible to characterize doublet tri-radicals by a heavy mixing of two doubly excited configurations in their CI wavefunction.

The PTSDW wavefunction (3.5) is an equal weighted superposition of the wavefunctions with  $A_1$  and  $B_2$  symmetries in the  $C_{2v}$  group around the axis  $\sigma_v$ :

$${}^2\Phi_{\text{PTSDW}} = \frac{1}{\sqrt{2}} ({}^2\Phi_{A_1} + i^2\Phi_{B_2}), \quad (3.8)$$

where

$$\left. \begin{aligned} {}^2\Phi_{A_1} &= \frac{1}{\sqrt{2}} \left\{ (1 + \cos \mu) |\phi_a \bar{\phi}_a \phi_a'| + (1 - \cos \mu) |\phi_a' \bar{\phi}_b \phi_b| \right. \\ &\quad \left. + \frac{1}{\sqrt{2}} \sin \mu (|\phi_a \bar{\phi}_b \phi_b| - |\phi_a \bar{\phi}_a' \phi_a'|) \right\}, \\ {}^2\Phi_{B_2} &= \frac{1}{\sqrt{2}} \left\{ (1 + \cos \mu) |\phi_a \bar{\phi}_a \phi_b| - (1 - \cos \mu) |\phi_a' \bar{\phi}_a' \phi_b| \right. \\ &\quad \left. + \frac{1}{\sqrt{2}} \sin \mu (|\phi_a \bar{\phi}_b \phi_a'| + |\phi_a \bar{\phi}_a' \phi_b|) \right\}. \end{aligned} \right\} \quad (3.9)$$

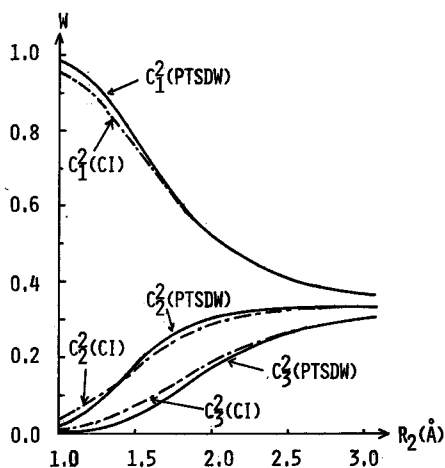


Fig. 7. The  $R_2$  dependences of the weights of the three configurations in the full CI ground state (---) and in the PTSDW state (—) at equilateral triangles.

Equation (3.8) with (3.9) indicates that the PTSDW state is a superposition of all of six linearly independent doublet RHF configurations which constitute  $E'$  representations of  $D_{3h}$  group.

We next consider the ASDW<sub>2</sub> state. From (2.3), the Slater determinant of ASDW<sub>2</sub> is expanded as

$$\begin{aligned} \Phi_{\text{ASDW}_2} = & \frac{1}{2} \{ (\cos \sigma + \cos \varphi) |\phi_a \bar{\phi}_a \phi_b| + (\cos \sigma - \cos \varphi) |\phi_a' \bar{\phi}_a' \phi_b| \\ & + (\sin \varphi - \sin \sigma) |\phi_a \bar{\phi}_a' \phi_b| + (\sin \varphi + \sin \sigma) |\phi_a' \bar{\phi}_a \phi_b| \}, \end{aligned} \quad (3.10)$$

where  $\varphi = (\omega^+ + \omega^-)/2$  and  $\sigma = (\omega^+ - \omega^-)/2$ . It is an eigenstate of  $S_z$  but not of  $S^2$ . We see from (3.10) that the doublet projected ASDW<sub>2</sub> (PASDW<sub>2</sub>) is of  $B_2$  symmetry in the  $C_{2v}$  group around the axis  $\sigma_v$  but not an irreducible representation of  $D_{3h}$  group. It is a superposition of the components with  $E'$  and  $A_2'$  symmetries:

$$\left. \begin{aligned} {}^2\Phi_{\text{PASDW}_2} &= N({}^2\Phi_{E'} + {}^2\Phi_{A_2'}), \\ {}^2\Phi_{E'} &= \frac{1}{2} \{ (\cos \sigma + \cos \varphi) |\phi_a \bar{\phi}_a \phi_b| + (\cos \sigma - \cos \varphi) |\phi_a' \bar{\phi}_a' \phi_b| \\ & \quad + \frac{1}{2} (\sin \varphi - \sin \sigma) (|\phi_a \bar{\phi}_b \phi_a'| + |\phi_a \bar{\phi}_a' \phi_b|) \}, \\ {}^2\Phi_{A_2'} &= 1/12 (3 \sin \varphi + \sin \sigma) (2 |\phi_a' \bar{\phi}_a \phi_b| + |\phi_a \bar{\phi}_a' \phi_b| - |\phi_a \bar{\phi}_b \phi_a'|), \end{aligned} \right\} \quad (3.11)$$

where  $N$  is a normalization factor. Due to the contamination of the component with wrong spatial symmetry, ASDW<sub>2</sub> is an inferior approximation to the TSDW solution.

The difference between the correlation effects incorporated into the TSDW and the ASDW solutions can also be analyzed in terms of the occupation number and the spin structure. The occupation numbers of the RHF orbitals (2.7) in the TSDW and the ASDW<sub>2</sub> states are given respectively by

$$\left. \begin{aligned} n_a^+ &= n_a^- = \frac{1}{2} (1 + \sin \mu), \\ n_a^+ &= n_a^- = n_b^+ = n_b^- = \frac{1}{4} (2 - \cos \mu), \end{aligned} \right\} \text{ for TSDW,} \quad (3.12)$$

$$\left. \begin{aligned} n_a^\pm &= \frac{1}{2} (1 + \cos \omega^\pm), \\ n_a^\pm &= \frac{1}{2} (1 - \cos \omega^\pm), \\ n_b^+ &= 1, \quad n_b^- = 0, \end{aligned} \right\} \text{ for ASDW}_2, \quad (3.13)$$

where  $n_i^\pm$  is the occupation number of the RHF orbital  $i$  with up or down spin. We show in Fig. 8 the  $R_2^-$  dependences of the occupation numbers. We see that the occupation numbers for the up and down spin orbitals are always the same in the TSDW state but not in the ASDW<sub>2</sub> state. Those of the orbitals  $\phi_a'$  and  $\phi_b$ , which constitute an  $E'$  representation of  $D_{3h}$  group, are also the same in the TSDW state but not in the ASDW<sub>2</sub> state. Therefore, up and down spin orbitals and the orbitals  $\phi_a'$  and  $\phi_b$  are respectively equivalent in the TSDW state but not in the ASDW<sub>2</sub> state. However, the total occupation numbers

$$n_{A_1'} = n_a^+ + n_a^-, \quad n_{E'} = n_a^+ + n_a^- + n_b^+ + n_b^-, \quad (3.14)$$

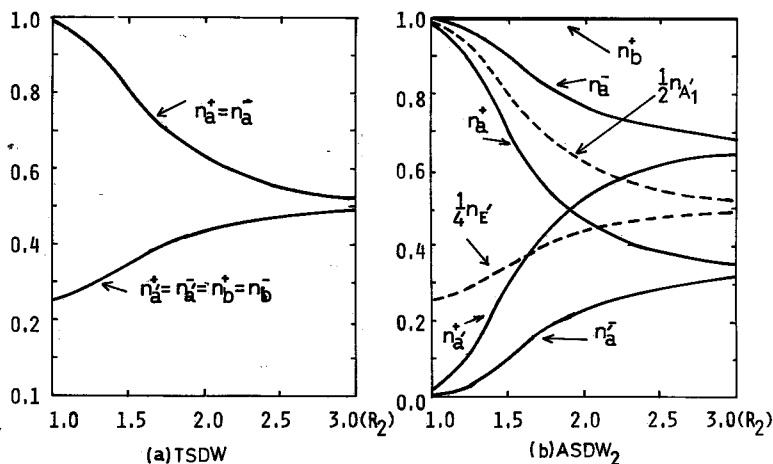


Fig. 8. The  $R_2$  dependences of the occupation numbers of the TSDW (a) and the ASDW<sub>2</sub> (b) states at equilateral triangles. For the ASDW<sub>2</sub> state, the total occupation numbers  $n_{E'}$  and  $n_{A_1'}$  are also indicated by the broken lines.

for the orbitals of  $A_1'$  and  $E'$  symmetries respectively behave quite similarly in the whole range of  $R_2$  for the TSDW and the ASDW<sub>2</sub> states as depicted in Fig. 8. This indicates that the Coulombic correlations incorporated into the TSDW and the ASDW<sub>2</sub> states are similar but the exchange correlations, which are mainly reflected in the spin structure of the states, incorporated into them are quite different. The energy gain due to the correlation is mainly brought about by the Coulombic correlation and the contribution of the exchange correlation is much smaller than it. This is the reason why the potentials of the TSDW and the ASDW states in  $D_{3h}$  conformations are similar in spite of a large difference in their occupation numbers for orbitals of different spins.

The difference in the exchange correlations incorporated into the TSDW and the ASDW states can be clearly demonstrated by their spin structures. It is to be noted that the spin structure of the TSDW state depicted in Fig. 5, should not be regarded as an approximation to the true spin density obtained from the first order density matrix of the true ground state. The TSDW state is neither an eigenstate of  $S_z$  nor any other component of  $S$ . As seen in Fig. 5, it interconnects the RHF<sub>1</sub> state with  $S_z = 1/2$  to the ASDW<sub>2</sub> state with  $S_z = -1/2$ . Such an interconnection is made possible through the broken  $S_z$  symmetry of the TSDW state. The first order spin density vectors on every atoms in the true ground state (3·1) are equivalent and directing along the  $z$  axis with the length  $1/3$ . The triangular spin structure of the TSDW state is apparently inconsistent with the first order spin structure of the true ground state. However, the spin correlation functions appear to have physical significance. The spin correlation functions for the TSDW and the ASDW<sub>2</sub> states are respectively given by

$$S_1 \cdot S_2 = S_2 \cdot S_3 = S_3 \cdot S_1 = -1/18 \cdot (1 + 2 \sin \mu)^2, \quad (3.15)$$

$$\left. \begin{aligned} S_1 \cdot S_2 &= \frac{1}{4}(1+k)^2, & S_2 \cdot S_3 &= S_3 \cdot S_1 = -\frac{1}{2}k(1+k), \\ k &= \frac{1}{3}(2\sqrt{2} \cos \varphi - \sin \varphi) \sin \sigma. \end{aligned} \right\} \quad (3.16)$$

In the TSDW state, all of the spin correlation functions have the same negative value indicating equivalence of the exchange interaction for all pairs of atomic spins in conformity with  $D_{3h}$  symmetry. The exchange interaction in the ASDW<sub>2</sub> state, on the other hand, is not isotropic in contradiction with  $D_{3h}$  symmetry. The spin correlation functions ( ${}^2\Phi_0 | S_i \cdot S_j | {}^2\Phi_0$ ) for the true ground state are of course isotropic and expected to be negative in sign. The quantum mechanical spin correlation function  $S_i \cdot S_j$  has a negative value  $-3/4$  for the pair of atoms making a singlet bond and a positive value  $1/4$  for the one making a triplet bond. In the equilateral  $H_3$  radical, each bond has more singlet character than triplet one as revealed by its valence bond structure. The isotropic and negative spin correlation functions in the TSDW state is at least qualitatively in agreement with those in the true ground state. Further discussion of the significance of the spin structure in UHF states will be given elsewhere.

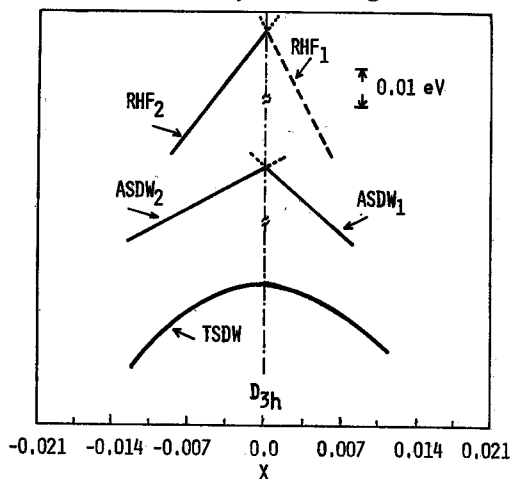


Fig. 9. The potentials of the UHF states for the deformation (3.17) from an equilateral triangle with  $R_0 = 1.5 \text{ \AA}$ . The total energies (eV) of the RHF, ASDW and TSDW solutions at the  $D_{3h}$  conformation are  $-51.546$ ,  $-53.709$  and  $-54.385$ , respectively.

We finally discuss the behavior of the UHF states in connection with Jahn-Teller's theorem.<sup>9</sup> We consider the small deformation of the equilateral  $H_3$  radical to  $C_{2v}$  conformation expressed with a parameter  $x$ , which is a normal coordinate of  $E'$  symmetry,<sup>14</sup> as

$$R_1 = \frac{\sqrt{3}}{2} R_0 (1-x), \quad R_2 = R_0 (1+x). \quad (3.17)$$

Two degenerate states of  $E'$  symmetry split into two states of  $A_1$  and  $B_2$  symmetries by the deformation from  $D_{3h}$  to  $C_{2v}$  conformation. The potentials of the  $A_1$  and  $B_2$  states have nonzero first order derivatives with respect to  $x$  at  $x=0$  with the same magnitude but of opposite signs. It is the characteristic property of the states forming a Jahn-Teller intersection at  $D_{3h}$ .<sup>9,14</sup>

We show in Fig. 9 the potentials of the RHF, ASDW and TSDW states for the deformation (3.17). The wavefunctions of RHF<sub>1</sub> and RHF<sub>2</sub> are of  $A_1$  and

$B_2$  symmetries respectively at  $C_{2v}$  and become degenerate and of  $E'$  symmetry at  $D_{3h}$  so that their potentials show a Jahn-Teller intersection.  $ASDW_1$  and  $ASDW_2$  are degenerate at  $D_{3h}$  but do not make exactly an  $E'$  representation. However, the doublet component of the  $ASDW_2$  wavefunction is of  $B_2$  symmetry as seen in (3.11) while that of  $ASDW_1$  contains a component of  $A_1$  symmetry which is not contained in  $ASDW_2$ . The difference in spatial symmetry of their doublet components leads to a Jahn-Teller like intersection of the  $ASDW_1$  and  $ASDW_2$  potentials. The potential of the TSDW state, on the other hand, shows no Jahn-Teller behavior and its first order derivative with respect to  $x$  is zero at  $D_{3h}$ . This is due to the fact that the doublet component of the TSDW wavefunction is an equal weighted superposition of the wavefunctions of  $A_1$  and  $B_2$  symmetries as shown in (3.8). The  $A_1$  and  $B_2$  components of the TSDW potential have non-zero first order derivatives but they exactly cancel out because of the equal weighted superposition of the two components. The situation is the same for the PTSDW state, and the projection to the doublet state is insufficient but a further projection to separate the  $A_1$  and the  $B_2$  spatial components is necessary to recover a Jahn-Teller behavior. Such a projection is easy for the present TSDW state. We obtain from (3.8)

$$\left. \begin{aligned} {}^2\Phi_{A_1} &= \frac{1}{\sqrt{2}} ({}^2\Phi_{PTSDW} + {}^2\Phi_{PTSDW}^*) \\ {}^2\Phi_{B_2} &= \frac{1}{i\sqrt{2}} ({}^2\Phi_{PTSDW} - {}^2\Phi_{PTSDW}^*) \end{aligned} \right\} \quad (3.18)$$

The spin- and space-symmetry projected TSDW states (3.18) will provide potentials exhibiting a Jahn-Teller intersection.

#### § 4. Discussion

We have indicated that the UHF ground state of the isosceles triangular  $H_3$  radical consists of the three "electronic phases", RHF<sub>1</sub>,  $ASDW_2$  and TSDW configurations. Use of GSO type orbitals is, therefore, inevitable in molecular orbital description of reacting systems in doublet ground state as well as singlet ground state discussed previously.<sup>9)</sup> Similar results may be obtained also for other three-electron systems such as allyl radical and cyclopropenyl radical in pi-electron approximation. The present result suggests that the UHF ground state of allyl radical with a flat triangular conformation should be  $ASDW_2$  type with spatial symmetry adapted DODS orbitals in agreement with previous UHF calculations.<sup>15), 16)</sup> The UHF ground state of cyclopropenyl radical with a  $C_{2v}$  conformation near an equilateral triangle, on the other hand, may be TSDW type if its Jahn-Teller distortion from  $D_{3h}$  conformation is small. A TSDW ground state arises in the radicals with degenerate or nearly degenerate half occupied and unoccupied RHF orbitals. Such a condition is fulfilled in the series of cyclic radicals  $C_3H_3$ ,  $C_5H_5$ ,  $C_6H_6^+$ ,  $C_7H_7$ ... if their Jahn-Teller distortions are small. Ovchinnikov et al.<sup>17)</sup> have

already shown that the UHF ground state of the Hubbard model of cyclic odd polyenic radicals is TSDW type with similar structure to Overhauser's helical spin density wave.<sup>19)</sup> As we have shown above, appearance of a TSDW ground state represents presence of a strong electronic correlation in the true ground state which produces an ordered spin correlation. It has been known that the cyclic radicals have ESR spectra with unusually large hyperfine coupling constants and  $g$  values<sup>19)~24)</sup> compared to the values estimated by the usual DODS theory.<sup>25)</sup> The expected strong spin correlation in the cyclic radicals might be the origin of their unusual ESR spectra.

We finally note importance of  $A_M$  instability in mechanistic characterization of radical reactions. An  $A_M$  instability of an ASDW or a doublet RHF ground state indicates either of a crossing of another state of different spin symmetry to the ground state, as illustrated for the internal rotation of ethylene,<sup>9)</sup> or appearance of a TSDW ground state, as illustrated for the  $H_4$ <sup>9)</sup> and the  $H_3$  systems. The TSDW ground state emerged from an  $A_M$  instability of an ASDW ground state interconnects it to another ASDW ground state with different spin structure as shown for the  $H_4$  and the  $H_3$  systems. Therefore, the  $A_M$  instability accompanied with appearance of a TSDW ground state represents a spin symmetry forbidden nature of the reaction path. Two ASDW states constructed from excitations of different symmetries have different spin structures and cannot be directly interconnected. The initial and the final ASDW states in a spin symmetry forbidden reaction path therefore involve different kinds of CI and are interconnected only through a TSDW state which involves both kinds of excitation and consequently both kinds of CI contained in the two ASDW states. Therefore, the spin symmetry forbidden reaction path is characterized by a change in the nature of the CI essentially contributing to the ground state and by the passage through a transition region where a complicated CI with a large mixing of at least two or more excited RHF configurations is essential in the ground state. The  $M$  instability of a TSDW ground state accompanied with appearance of a TSW ground state, which may occur in chemical reactions as illustrated for the  $H_4$  system,<sup>9)</sup> also represents another kind of spin symmetry forbidden reaction path which involves a more complicated conversion process in the nature of CI in the ground state than in the case of an  $A_M$  instability of an ASDW state.

The present UHF theoretical criterion for the spin symmetry selection rule supports the selection rule based on a simple Heisenberg model proposed recently by one of the authors.<sup>26)</sup> However, it is to be noted that the Heisenberg model can be applied only to the radicals in which the correlation is so strong that localized spin moments are well developed.

#### Acknowledgement

The authors wish to thank Mr. T. Takabe for his aid in programming of a GSO UHF computer program.



References

- 1) H. Fukutome, *Prog. Theor. Phys.* **47** (1972), 1156.
- 2) H. Fukutome, *Prog. Theor. Phys.* **49** (1973), 22.
- 3) H. Fukutome, *Prog. Theor. Phys.* **50** (1973), 1433.
- 4) K. Yamaguchi, T. Fueno and H. Fukutome, *Chem. Phys. Letters* **22** (1973), 461.
- 5) H. Fukutome, M. Takahashi and T. Takabe, *Prog. Theor. Phys.* **53** (1975), 1580.
- 6) H. A. Jahn and E. Teller, *Proc. Roy. Soc.* **A161** (1937), 220.
- 7) H. Fukutome, *Prog. Theor. Phys.* **52** (1974), 115.
- 8) H. Fukutome, *Prog. Theor. Phys.* **52** (1974), 1766.
- 9) J. A. Pople and G. A. Segal, *J. Chem. Phys.* **43** (1965), S136.
- 10) J. Paldus and J. Čížek, *J. Chem. Phys.* **52** (1970), 1.
- 11) R. W. Patch, *J. Chem. Phys.* **59** (1973), 6468.
- 12) E. F. Hayes and A. K. O. Siu, *J. Am. Chem. Soc.* **93** (1971), 2090.
- 13) L. Salem and C. Rowland, *Angew. Chem. intern*, Ed **11** (1972), 92.
- 14) R. N. Porter, R. M. Stevens and M. Karplus, *J. Chem. Phys.* **49** (1968), 5163.
- 15) A. D. McLachlan, *Mol. Phys.* **3** (1960), 233.
- 16) A. Laforgue, J. Čížek and J. Paldus, *J. Chem. Phys.* **59** (1973), 2560.
- 17) A. A. Ovchinnikov, I. I. Ukrainski and G. V. Kventsel, *Soviet Phys.-Uspekhi* **15** (1973), 575, and references cited therein.
- 18) A. W. Overhauser, *Phys. Rev.* **128** (1962), 1437.
- 19) G. Cirelli, F. Graf and Hs. H. Gunthard, *Chem. Phys. Letters* **28** (1974), 494.
- 20) H. J. Silverstone, D. E. Ward and H. M. McConnell, *J. Chem. Phys.* **42** (1965), 3931.
- 21) G. R. Liebling and H. M. McConnell, *J. Chem. Phys.* **42** (1965), 3931.
- 22) P. J. Krusic and J. K. Kochi, *J. Am. Chem. Soc.* **90** (1968), 7155.
- 23) B. Segal, M. Kaplan and G. K. Frankel, *J. Chem. Phys.* **43** (1965), 4191.
- 24) M. K. Carter and G. Vincow, *J. Chem. Phys.* **47** (1967), 292.
- 25) J. A. Pople, D. L. Beveridge and P. A. Dobosh, *J. Am. Chem. Soc.* **90** (1968), 4201.
- 26) K. Yamaguchi, *Chem. Phys. Letters* **28** (1974), 93.